IN VIVO *39*: 1786-1798 (2025)
doi: 10.21873/invivo.13980

Controlling Cellular Behavior by Surface Design of Titanium-based Biomaterials

TONYA ANDREEVA[1], OSMAN AKBAS[2], ANNE JAHN[3], ANDREAS GREULING[2], ANDREAS WINKEL[2], MEIKE STIESCH[2] and RUMEN KRASTEV[1]

[1]Reutlingen University, Faculty Life Sciences, Reutlingen, Germany;
[2]Hannover Medical School, Department of Prosthetic Dentistry and Biomedical Materials Science, Hannover, Germany;
[3]Laser Zentrum Hannover e.V., Hannover, Germany

Abstract

Background/Aim: Titanium alloys, especially Ti_6Al_4V, are widely used in orthopedic and dental implants. Additive manufacturing has emerged as an innovative fabrication technique for titanium implants, gradually replacing traditional machining methods. A notable feature of additively manufactured medical devices is their considerable surface heterogeneity and roughness. Coating these materials to achieve physical and chemical uniformity is essential for enhancing biocompatibility. This study evaluates the combined effect of surface roughness (ranging from sub-micrometer to micrometer scale) and three nanometer-thick polyelectrolyte multilayer coatings on protein adsorption, as well as the adhesion and proliferation of normal human osteoblasts.

Materials and Methods: The adhesion of human osteoblasts to various substrates (either uncoated or coated) was quantified using a lactate dehydrogenase assay and scanning electron microscopy. The surface density of adsorbed human serum albumin was analyzed by the Bradford assay.

Results: Application of polyelectrolyte multilayer coatings significantly increased the hydrophilicity of titanium substrates without altering their sub-micrometer and micrometer roughness or topography. The coatings rich in reactive amino groups were found to enhance the adsorption of human serum albumin and promote the adhesion of osteoblasts.

Conclusion: The chemical composition of the surface, particularly the presence of free primary amino groups, significantly affects cellular behavior in machined, sand-blasted, and additively manufactured titanium materials, while the impact of surface roughness appears secondary. No correlation was observed between surface hydrophilicity and protein adsorption or cell attachment.

Keywords: Titanium alloys, additive manufacturing, implant surface roughness, surface modification, polyelectrolyte multilayer coatings, biomaterials, human osteoblasts adhesion and proliferation.

Tonya Andreeva, Reutlingen University, Faculty Life Sciences, Alteburgstrasse 150, 72762 Reutlingen, Germany. E-mail: tonya.andreeva@reutlingen-university.de

Received November 16, 2024 | Revised December 9, 2024 | Accepted December 12, 2024

Introduction

Qualitative and quantitative studies on the osteointegration of bone implants from various materials (mostly ceramics, metals, and polymers/bone cements) have been conducted since the mid-twentieth century (1). After approximately 30 years, the first studies on the influence of material surface properties on osteointegration emerged (2). Since then, extensive research has focused on how the chemical composition of a surface, its topography, roughness, hydrophilicity (surface energy) and stiffness affect bone-to-implant contact. The primary aim has been to mitigate the formation of a fibrous layer that impedes osteointegration, as well as to prevent surrounding bone degradation and loosening of the implant (3). Among all surface modifications, roughness and topology were found to play a pivotal role (4, 5).

Numerous studies have demonstrated that roughening the titanium surface of dental implants enhances their mechanical fixation to bone; however, the efficacy of their biological fixation remains uncertain (6-9). A recent systematic review involving 362 sand-blasted and 360 machined implants borne in upon healthy subjects revealed that sandblasting outperforms machined surfaces in terms of implant failure rates, but no significant difference was observed in marginal bone loss between the two types of implants (10).

The degree of average surface roughness (Sa) has been shown to influence various aspects of osteointegration. Nanoscale roughness (<100 nm) optimizes protein adsorption, which promotes osteoblast adhesion and enhances the interaction between mineralized bone and the surface of the implant (11). However, some studies challenge this notion, indicating that variations in nano-roughness did not yield statistically significant differences in the adhesion of mouse pre-osteoblastic cells (MC3T3-E1 line) (12) and bone marrow-derived stem cells (13). In contrast, micrometer and sub-micrometer roughness (up to 2 μm) enhance the alignment of osteocytes and protrusion in their dendrimers into the surface structures, thereby improving primary implant fixation and ensuring long-term mechanical stability (11). Recently, additively manufactured dental implants, commonly produced through 3D printing, have been growing popularity in the field of dentistry (14). There are several factors contributing to this. The technology ensures (i) a high level of customization by fitting to each patient's specific anatomical structure, thus making the implants more comfortable and effective; (ii) complex designs by enabling the fabrication of complex geometries that are impossible or difficult to create with existing methods – therefore, additive manufacturing improves both functionality and aesthetic appeal; (iii) biocompatibility to guarantee patient safety and implantation success as advanced materials utilized in 3D printing are engineered to be biocompatible (14).

Modifying the chemical composition of an implant's surface allows for further optimization in the development of biomaterials by improving surface functionality of the implant surface while maintaining the mechanical properties and topography. Surface chemical modification is typically accomplished by applying a layer of material (a coating) that differs from the base material of the implant, often titanium (Ti) in the case of bone substitutes.

Layer-by-layer assembled polyelectrolyte multilayers (PEMs) are nanometer-thin polymer coatings with highly tunable surface and bulk properties. They consist of at least one polyanion and one polycation, known as a polyelectrolyte pair. The layer building process is electrostatically driven. The stability of the coatings is given by the strong entropy changes upon the adsorption. This allows for the modulation and tailoring of the multilayer properties based on the choice of polyelectrolytes and the adjustment of deposition conditions. PEMs, created from a wide range of both synthetic and naturally derived polyelectrolytes, are increasingly used as coatings and have been shown to either promote or inhibit adhesion, viability, differentiation, and migration of various cell types, including osteoblasts (15, 16).

This study investigated the effect of Sa, as well as physicochemical properties, of standard-machined (MTi), sandblasted (SBTi), and additively manufactured (AMTi) Ti_6Al_4V (Grade 23) materials, bare or modified with three

types of PEM, on protein adsorption, human osteoblast (NHOst) adhesion and proliferation *in vitro*. These materials are intended for dental implant applications and their roughness ranges between sub-micrometer and micrometer. The choice of polyelectrolyte pairs used in PEM fabrication determines their surface and bulk properties, influencing cellular adhesion to PEM-coated materials, which can range from cytophilic to cytophobic (15). The coatings used here included one bioinspired formulation of hyaluronic acid (HA)/chitosan (Chi) and two synthetic pairs: polyacrylic acid (PAA)/polyallylamine hydrochloride (PAH) and polystyrene sulfonate (PSS)/PAH. These coatings, characterized by nanoscale thickness and minimal roughness, impart their unique physicochemical properties to the titanium surfaces without altering their underlying roughness.

Materials and Methods

Manufacturing of AMTi substrates. The industrial machine Lasertec 12 SLM from DMG MORI at Laser Zentrum Hannover e.V. (LZH) (Hannover, Germany) was utilized to additively manufacture the titanium specimens through the powder bed fusion laser-based technique. The apparatus was equipped with a 400 W fiber laser that operates in continuous wave mode at 1070 nm, with a minimum spot diameter of 35 µm. Particle sizes ranged from 20.0 to 53.0 µm, and the powder standard used was Ti_6Al_4V Grade 23 from ECKART TLS GmbH (Bitterfeld-Wolfen, Germany). The powder had a mostly spherical morphology. The manufactured specimen had the following design specifications: 12 mm diameter and 2 mm thickness. Using a contour-hatch scan strategy, all specimens were created upright. To achieve different roughness, the laser parameters of the contour were varied (power: 200/120/40 W and speed: 1,000/1,200/287 mm/s). For the manufacturing of the hatch, a laser power of 175 W and 1050 mm/s was chosen).

Following the production procedure and ultrasonic cleaning, further heat treatment was carried out in order to guarantee a homogeneous and stable microstructure based on ISO20160 (17) and to minimize residual stresses associated to manufacturing. The heat treatment took place in a vacuum furnace for 4 h at 1,050˚C (18).

Machined samples and mechanical surface modification by sand-blasting. From a Ø12 mm titanium rod (Grade 23, L. Klein AG, Biel, Switzerland) 2 mm thick sample disks were cut using a linear precision saw (Brillant 220; ATM Qness GmbH, Mammelzen, Germany) with a diamond cutting disc (Buehler, Leinfelden-Echterdingen, Germany). The samples were deburred afterwards in a rotary tumbler (Model 45C; Lortone Inc., Mukilteo, WA, USA).

A sandblasting machine from previous work was used (19) to process the cut disks for the sandblasted samples. Corundum particles (SHERA Werkstoff-Technologie GmbH, Lemförde, Germany) with a nominal grain size of 110 µm were used as the abrasive medium. The samples were prepared with a sandblasting angle of 45˚, a distance of 10 mm and a pressure of 2 bar. Each sample underwent this process for 8 min as a result of the path distance of 0.3 mm and forward speed 1 mm/s, following a meander-shaped sandblasting path.

The arithmetic mean Sa of the samples was measured at the center of the sandblasted surface over an area of 10.24 mm^2 (3.2 mm×3.2 mm) with 640,000 data points within this area (800×800). This measurement was performed on three specimens for each surface type using an optical profilometer (MicroProf 100; FRT GmbH, Bergisch-Gladbach, Germany).

Surface modification by PEMs. All polyelectrolytes, namely poly(ethylene imine) (PEI; 750 kDa, 50% wt; Sigma-Aldrich, Steinheim, Germany), PSS (70 kDa; Sigma-Aldrich, Steinheim, Germany), PAA (100 kDa, 35% wt; Sigma-Aldrich), PAH (120-200 kDa; Life Technologies GmbH, Darmstadt, Germany), chitosan (50-190 kDa, 75-85% deacetylated; Sigma-Aldrich), and HA (360 kDa; Lifecore Biomedical, LLC, Chaska, MN, USA), were used as received.

Three types of PEMs composed of five different polyelectrolytes were applied here – $(PSS/PAH)_5$, $(PAA/PAH)_5$ and $(HA/Chi)_5$. The PEM coatings were

assembled layer-by-layer by dip coating technology following the protocol described in (20). An ensemble of five bilayers was chosen to ensure that the PEM coating was homogeneous and unaffected by the type and properties of the substrate (21). A monolayer of branched PEI was applied as anchoring layer to improve the adhesion of the PEM to the substrate (22).

The coatings for the physicochemical characterization were constructed on Si wafers [crystal orientation (100), 10 mm×10 mm; CrysTec GmbH, Berlin, Germany] pre-cleaned by successive ultrasonication in acetone and isopropanol (both for 2 min). The coatings for cell culture experiments were deposited in sterile conditions on MTi, SBTi and AMTi disks sequentially cleaned in a hot (60˚C) solution of 10 mM sodium dodecyl sulfate (for 15 min), acetone and isopropanol (both for 2 min under sonication).

The thickness of the coatings was assessed by spectroscopic multiangle ellipsometer (SE 400adv PV; Sentech, Berlin, Germany). The hydrophilicity was determined using optical contact angle measurement of static water drop and contour analysis system (DataPhysics, Filderstadt, Germany). Atomic force microscopy (Innova Bruker Inc., Billerica, MA, USA) was used in tapping mode to evaluate the Sa of PEM coatings on Si wafers. The surface density of adsorbed human serum albumin (HSA; Sigma-Aldrich) was assessed by incubation of the uncoated and PEM-coated substrates for 2 h with a 100 μg/ml solution of HSA in Tris buffer (pH 7.4) (Sigma-Aldrich). The residual concentration of HSA in the solution after incubation was analyzed by following the Bradford assay (23). Each sample was prepared in triplicate, and each test was performed a minimum of three times for each sample type.

Cell adhesion and proliferation. A modified lactate dehydrogenase activity (LDH) assay was used to evaluate the adhesion and proliferation of human osteoblasts on polymer coatings in comparison to uncoated titanium alloy disks, as described elaborately for different cell types in previous publications (24-27). Briefly, the coated and uncoated specimens were covered with human osteoblasts (NHOst; Lonza, Basel, Switzerland) at a density of 10,000 cells/cm^2. After an incubation period of 24 or 72 h, the samples were washed with phosphate-buffered saline (PBS) (Biochrom AG, Berlin, Germany) to remove unattached cells. The adherent cells were completely lysed using 10% Triton-X-100 (Sigma-Aldrich) at 37˚C for 30 min. Lactate dehydrogenase concentration was measured in each lysate using a Cytotoxicity Detection Kit (Roche Diagnostics GmbH, Mannheim, Germany). The number of adherent osteoblasts was calculated through comparison with a corresponding standard curve. An analysis of variance test was used to determine the statistical differences between results from cell adhesion and proliferation studies.

Cell morphology. Titanium samples were rinsed with PBS and fixed for 4 h in 0.1% glutaraldehyde and 4% paraformaldehyde diluted in 200 mM HEPES buffer (Sigma-Aldrich, St. Louis, MO, USA). Specimens were dehydrated in graded ethanol solutions before performing chemical drying with hexamethyldisilazane (Sigma-Aldrich Chemie GmbH, Taufkirchen, Germany). For scanning electron microscopy (SEM), samples were mounted on stubs, sputtering coated (Quorum Q150R ES, Laughton, Quorum Technologies, Lewes, UK) with a thin layer of gold (sputter time 300 s) and imaged using an SE1 detector on an EVO MA10 SEM (Carl Zeiss, Oberkochen, Germany) at 15 kV.

Results

The topography of the titanium substrates revealed by SEM was diverse (Figure 1).

The machined titanium disks (MTi) exhibited a smooth surface with parallel grooves oriented anisotropically (Figure 1A), yielding a mean (±standard deviation) Sa of 0.50±0.05 μm, which aligns with literature values for similar surfaces (28). In contrast, SBTi surfaces displayed an irregular rough topography characterized by spike-like structures (Figure 1B), resulting in an Sa of 2.06±0.04 μm.

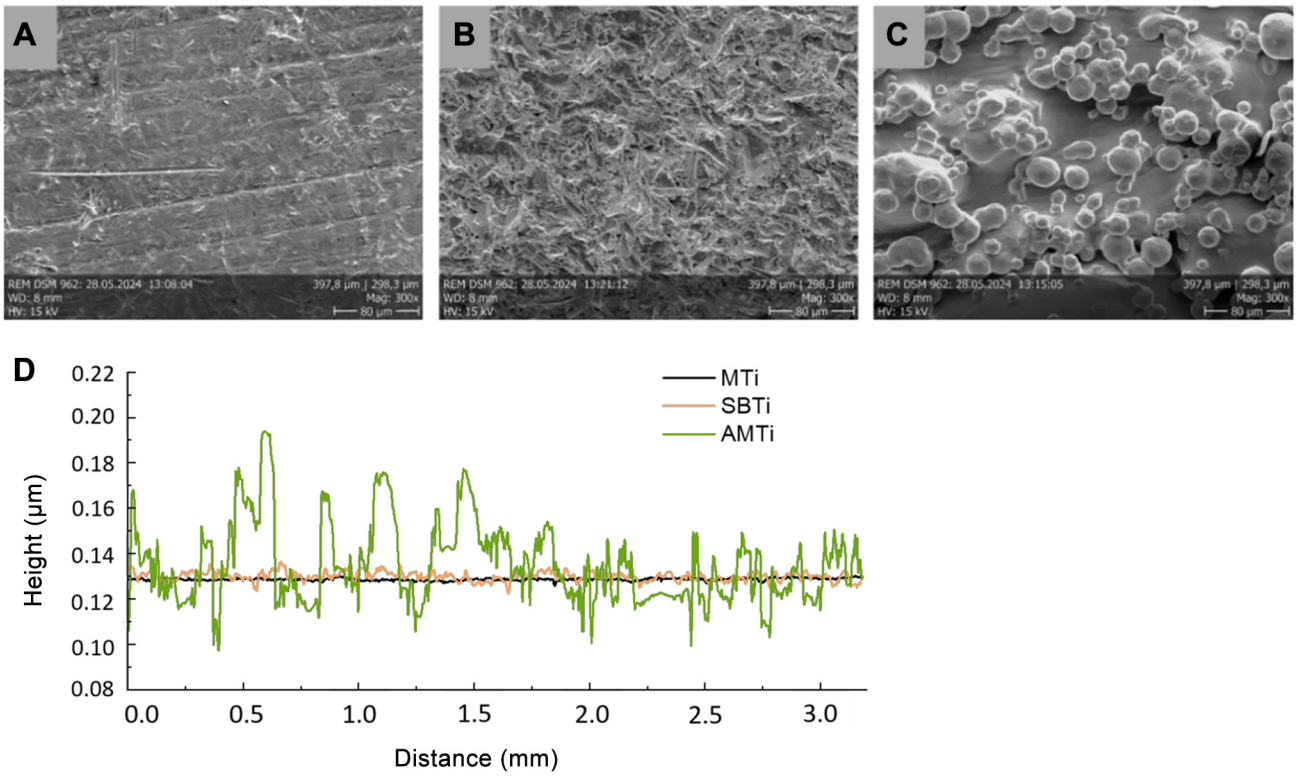

Figure 1. *Scanning electron micrographs of (A) machined titanium (MTi), (B) sand-blasted titanium (SBTi), and (C) additively manufactured titanium (AMTi) disks with roughness profiles (D) obtained with an optical profilometer.*

This roughness increased the real surface area by a factor of 1.2 compared to the projected area (Table I). The AMTi disks featured a complex microstructured surface with isotropic irregularities, formed by partially melted titanium alloy powder particles (Figure 1C). The average roughness of AMTi disks was estimated at 14.64±1.20 µm, significantly increasing the real surface area by a factor of 3.1 (Table I).

The surface properties of PEM coatings applied to model silicon wafers are summarized in Table II. A key limitation of ellipsometry is that the sample surface must be flat and smooth, ideally with a roughness of less than 50 nm (29), which makes the Ti_6Al_4V substrates not applicable. Polished monocrystalline Si substrates were selected due to their nearly perfect smoothness, exhibiting Sq roughness of 0.28±0.05 nm (30) and a well-defined, homogeneous surface chemical composition. All three coatings were only nanometer-thick and moderately hydrophilic. Consistent with their low thickness, the average roughness of the coatings was minimal, approaching that of commercial tissue culture plastic (TCP) (31). Referring to published studies, the thickness

Table I. *Arithmetic mean surface roughness (Sa), projected area and true surface area of the various Ti_6Al_4V disks. Data are presented as the mean value±standard deviation obtained from three samples, each analyzed at three spots.*

Surface	Sa, µm	Projected area, mm^2	True surface area, mm^2
MTi	0.50±0.05	1.00	1.04±0.01
SBTi	2.06±0.40	1.00	1.19±0.14
AMTi	14.64±1.20	1.00	3.12±0.05

AMTi: Additively manufactured titanium; MTi: machined titanium; SBTi: sand-blasted titanium.

Table II. *Thickness and roughness of the polyelectrolyte multilayer coatings applied on model Si wafers. Data are presented as the mean value±standard deviation obtained from three samples, each analyzed at three spots.*

Coating applied	Thickness, nm	Sa, nm	Sq, nm
$(PSS/PAH)_5$	15.6±0.2	2.6±0.2	2.8±0.3
$(PAA/PAH)_5$	12.2±2.1	1.7±0.4	1.4±0.4
$(HA/Chi)_5$	10.1±0.1	3.2±0.4	3.5±0.7

Chi: Chitosan; HA: hyaluronic acid; PAA: polyacrylic acid; PAH: polyallylamine hydrochloride; PSS: polystyrene sulfonate; Sa: average surface roughness; Sq: root mean square roughness.

Table III. *Average water contact angles of Si wafers and Ti_6Al_4V disks with three different surface roughness values, without a coating, and with polyelectrolyte multilayer coatings. Data are presented as the mean value±standard deviation obtained from three samples, each analyzed at three spots.*

	Average water contact angle			
Coating applied	Si wafer	MTi	SBTi	AMTi
None	64±3°	73±3°	99±2°	67±3°
$(PSS/PAH)_5$	71±2°	55±8°	46±3°	3±7°
$(PAA/PAH)_5$	73±2°	45±8°	66±7°	23±3°
$(HA/Chi)_5$	67±2°	54±4°	52±2°	65±8°

AMTi: Additively manufactured titanium; Chi: chitosan; HA: hyaluronic acid; MTi: machined titanium; PAA: polyacrylic acid; PAH: polyallylamine hydrochloride; PSS: polystyrene sulfonate; SBTi: sand-blasted titanium.

of PEM on the MTi, SBTi and AMTi substrates can be expected to be higher than on model Si substrates (30). On the one hand, the thickness of PEM was shown to increase with the roughness of the substrate (22), on the other hand to depend on the chemical nature of the substrate (30). The thickness of $(PAH/PAA)_5$ multilayers on Ti wafers was reported to be three times greater than that on Si wafers, despite both substrates being single-sided polished and having similar roughness (30).

Surface roughness contributes to material wettability, therefore we assessed the intrinsic hydrophilicity of PEM coatings on model Si substrates, as well as on uncoated and PEM-coated MTi, SBTi and AMTi disks, by measuring the water contact angle (Table III). All PEM coatings and uncoated substrates were hydrophilic, except the uncoated SBTi, which was hydrophobic with a contact angle of 99°. It is nearly impossible to alter surface micro-morphology without simultaneously affecting the chemical composition of the surface. Therefore, we attribute the enhanced hydrophobicity of SBTi substrates to alterations in surface chemistry caused by residues from the Al_2O_3 particles used in the sand-blasting process, which has been demonstrated to reduce surface hydrophilicity (32). Uncoated MTi disks were slightly less hydrophilic than Si wafers, in agreement with the findings of Mesić *et al.* (30). The PEM-coated MTi disks exhibited moderate hydrophilicity, as evidenced by contact angles that were lower than those observed for the corresponding Si wafers, likely due to the increased Sa of the MTi substrates. Increasing Sa had a PEM-dependent effect on contact angle. Wenzel's basic rule accounting for the effect of Sa on wettability, states that the apparent contact angle of a smooth hydrophilic surface decreases with increasing Sa (33). However, many experimental exceptions to this rule have been reported. For instance, plasma-treated and grounded/roughened TCP, which has an average Sa of 2.365 μm, exhibits a significantly higher water contact angle compared to the original non-grounded TCP with an average Sa of 19 nm, regardless of whether the original smooth surface was hydrophilic or hydrophobic (34). Among our data, only the $(PSS/PAH)_5$-coated samples conformed to Wenzel's rule, demonstrating an increase in hydrophilicity with Sa and reaching superhydrophilicity at AMTi (Table III). The uncoated Ti_6Al_4V disks exhibited a peak in contact angle at moderate roughness (SBTi), and a similar trend was observed for the $(PAA/PAH)_5$-coated samples. No statistically significant effect of Sa on the hydrophilicity of $(HA/Chi)_5$-coated Ti_6Al_4V disks was observed. More importantly, the application of PEM coatings significantly increased the hydrophilicity of MTi, SBTi, and AMTi surfaces without altering their sub-micrometer and micrometer roughness or topography.

The surface density of HSA adsorbed onto uncoated titanium disks, as well as on the PEM coatings and the TCP used as a control substrate for cell studies, is summarized

in Table IV. For each substrate type, the HSA surface density follows the order: PSS/PAH-coated>PAA/PAH-coated>uncoated>HA/Chi-coated. The three-fold increase in the effective surface area of AMTi, due to its high Sa (see Table I), resulted in a three- to five-fold increase in the amount of adsorbed HSA compared to the smooth MTi surface, depending on the coating applied. AMTi substrates offer a greater number of active sites, along with structure-specific corners and holes that facilitate protein accommodation.

The adhesion of NHOst cells to various substrates (either uncoated or PEM-coated) was quantified using a LDH assay, with results normalized to those on TCP plastic. Figure 2 summarizes the results of the attachment efficiency of NHOst on different treated surfaces. Initial adhesion of cells was influenced solely by surface chemical composition (*i.e.*, the type of PEM coating applied), rather than the Sa of the titanium substrates. Cell adhesion was suppressed on all uncoated and PEM-coated titanium surfaces compared to TCP, except for the PSS/PAH-coated SBTi, which showed adhesion levels comparable to TCP.

Regarding the smooth MTi substrates, NHOst cells adhered statistically equally to uncoated, PSS/PAH-coated, and PAA/PAH-coated surfaces, but adhesion was reduced by 50% on HA/Chi-coated substrates. The reduced cell attachment on HA/Chi coatings aligns with previous studies involving various cell types, including HCS-2/8 human chondrosarcoma cells (35), A549 human lung carcinoma epithelial cells, baby hamster kidney fibroblasts, C2C12 mouse myoblasts, and MC-3T3-E1 murine osteoblasts (36). These studies collectively demonstrate the anti-adhesive properties of this coating.

PSS/PAH and PAA/PAH coatings statistically significantly improved the initial attachment of NHOst on SBTi, by 60% and 40% respectively. The HA/Chi coating lowered cell adhesion by 21% relative to uncoated SBTi. The cell adhesion on AMTi was similar to those on SBTi. There were 50% more cells adhered to PSS/PAH-coated compared to the uncoated AMTi. The adhesion capacity of PAA/PAH- and HA/Chi-coated AMTi surfaces was statistically indistinguishable from those on uncoated surfaces.

Table IV. *Surface density of human serum albumin (HSA) adsorbed on uncoated Ti_6Al_4V disks with different roughness, tissue culture plastic (TCP) and disks with polyelectrolyte multilayer coatings. Data presented are the mean value±standard deviation, obtained from three samples.*

	Surface density of HSA (μg/cm^2)			
Coating applied	TCP	MTi	SBTi	AMTi
None	0.60±0.08	0.05±0.02	0.05±0.03	0.16±0.01
$(PSS/PAH)_5$	0.98±0.08	0.30±0.05	0.35±0.07	0.96±0.13
$(PAA/PAH)_5$	0.71±0.10	0.16±0.03	0.18±0.04	0.49±0.05
$(HA/Chi)_5$	0.14±0.06	0.01±0.01	0.02±0.01	0.05±0.04

AMTi: Additively manufactured titanium; Chi: chitosan; HA: hyaluronic acid; MTi: machined titanium; PAA: polyacrylic acid; PAH: polyallylamine hydrochloride; PSS: polystyrene sulfonate; SBTi: sand-blasted titanium.

Cell proliferation was highest on TCP and comparably high only for cells grown on uncoated MTi, as well as MTi coated with PSS/PAH (Figure 2). On uncoated Ti-disks, NHOst proliferation decreased significantly with increasing Sa, while on AMTi the number of cells after 72 h just equaled that at 24 h. The inverse relation between micrometer-scale Sa and osteoblast proliferation shown here has been previously demonstrated (37). Application of PSS/PAH coating did not affect the cell proliferation on MTi but suppressed it on SMTi and AMTi, with even a trend to cell loss. It is worth mentioning that the proportion of cells on PSS/PAH-coated AMTi at 72 h was still 35% higher compared to uncoated Ti_6Al_4V substrates. Application of PAA/PAH and HA/Chi coatings led to cell loss on all Ti_6Al_4V substrates to a similar degree regardless of Sa.

The ranking of all 12 studied Ti_6Al_4V samples, which had three roughness levels and included both uncoated and coated samples with three PEM coatings, is clearly outlined in Table V based on their ability to support cell viability.

In summary, the adhesion of NHOst cells to Ti_6Al_4V surfaces increased in the order: PSS/PAH-coated≥PAA/PAH-coated≥uncoated>HA/Chi-coated (Table V).

NHOst adhered to smooth MTi (Figure 3) and to moderately rough SMTi showed better spreading compared

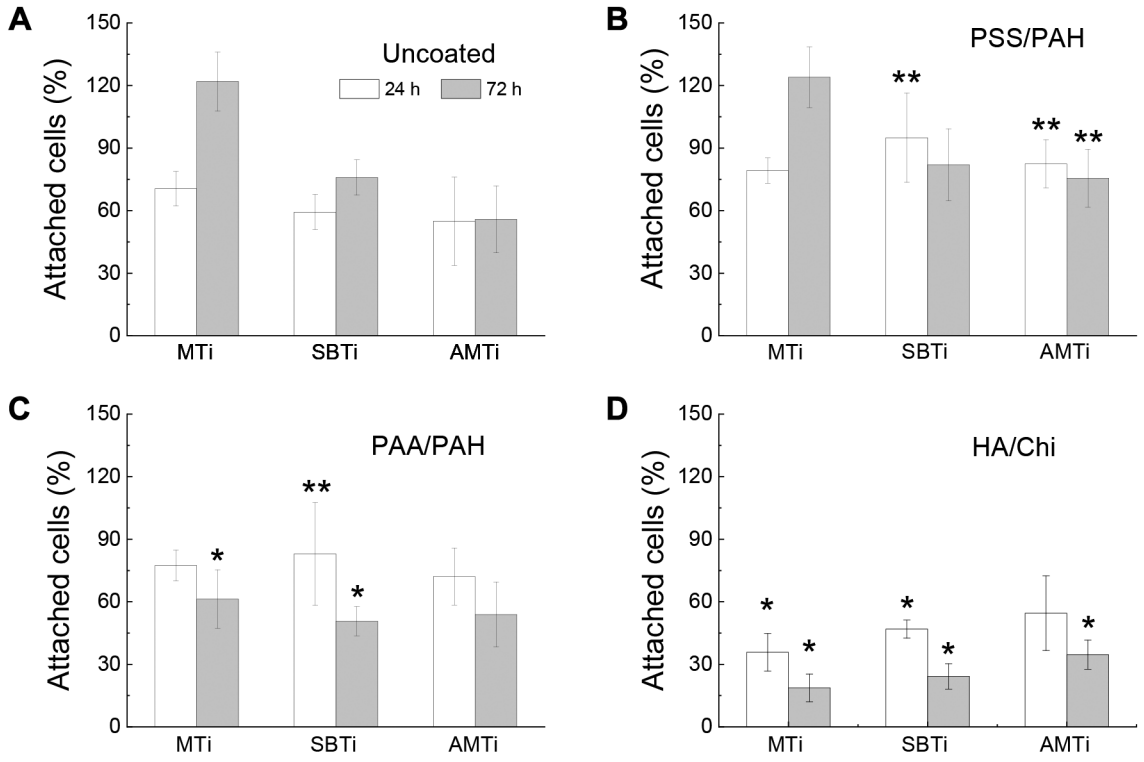

Figure 2. *Proportion of attached human osteoblasts after 24 h of cultivation, reflecting the extent of cell adhesion, and after 72 h of cultivation, reflecting the extent of cell proliferation, examined on machined (MTi), sand-blasted (SBTi), and additively manufactured (AMTi) titanium disks, uncoated (A) and coated with polystyrene sulfonate (PSS)/polyallylamine hydrochloride (PAH) (B), polyacrylic acid (PAA)/PAH (C), and hyaluronic acid (HA)/chitosan (Ch) (D). *Significantly different at p<0.05, **p<0.01 from the control uncoated Ti_6Al_4V of the same type. The data presented are averages obtained from eight samples.*

to AMTi. SEM images revealed that the cells on the surface of the uncoated, PSS/PAH-coated and on PAA/PAH-coated MTi and SBTi were completely flattened and fully extended, therefore closely adhering to the surface. Moreover, they were confluent and connected to adjacent cells *via* extended filamentous pseudopods. Cells grown on the AMTi substrates exhibited a more rounded cell body with thin and long filopodia extending between the Ti grains covering the surface of the disks. Some cells were not even adherent, but instead were just hanging by their filopodia, attached to the surrounding Ti particles. No morphological changes of the cells were observed due to the coating of MTi- and SBTi-substrates with PSS/PAH and PAA/PAH; however, on HA/Chi-coated surfaces, the cells appeared rounder or even detached.

Discussion

Numerous studies have described the impact of Sa on cell adhesion, proliferation, viability, migration, and differentiation (4, 5, 38, 39). However, despite the extensive data available, these studies often yield conflicting results. This inconsistency may originate from variations in the ranges of nano- and micro-roughness, surface topographies, materials used, and the types of cells examined. In this study, we focused on the effect of Sa of Ti alloy materials at the sub micrometer to micrometer scale on the adhesion and proliferation of human osteoblasts (NHOst).

The relationship between the surface properties of materials and cellular behavior is complex. Upon implantation, the surface of an implant is initially covered

Table V. *Ranking of the investigated Ti_6Al_4V substrates with three roughness levels, uncoated and coated with three polyelectrolyte multilayer coatings, according to their ability to support cell attachment.*

	Cell attachment ranking, best first	
Ti_6Al_4V substrate	At 24 h	At 72 h
MTi	Uncoated=PSS/PAH=PAA/PAH>HA/Chi	Uncoated=PSS/PAH>PAA/PAH>HA/Chi
SBTi	PSS/PAH>PAA/PAH>Uncoated>HA/Chi	Uncoated=PSS/PAH>PAA/PAH>HA/Chi
AMTi	PSS/PAH>PAA/PAH>Uncoated>HA/Chi	PSS/PAH>Uncoated=PAA/PAH>HA/Chi

AMTi: Additively manufactured titanium; Chi: chitosan; HA: hyaluronic acid; MTi: machined titanium; PAA: polyacrylic acid; PAH: polyallylamine hydrochloride; PSS: polystyrene sulfonate; SBTi: sand-blasted titanium.

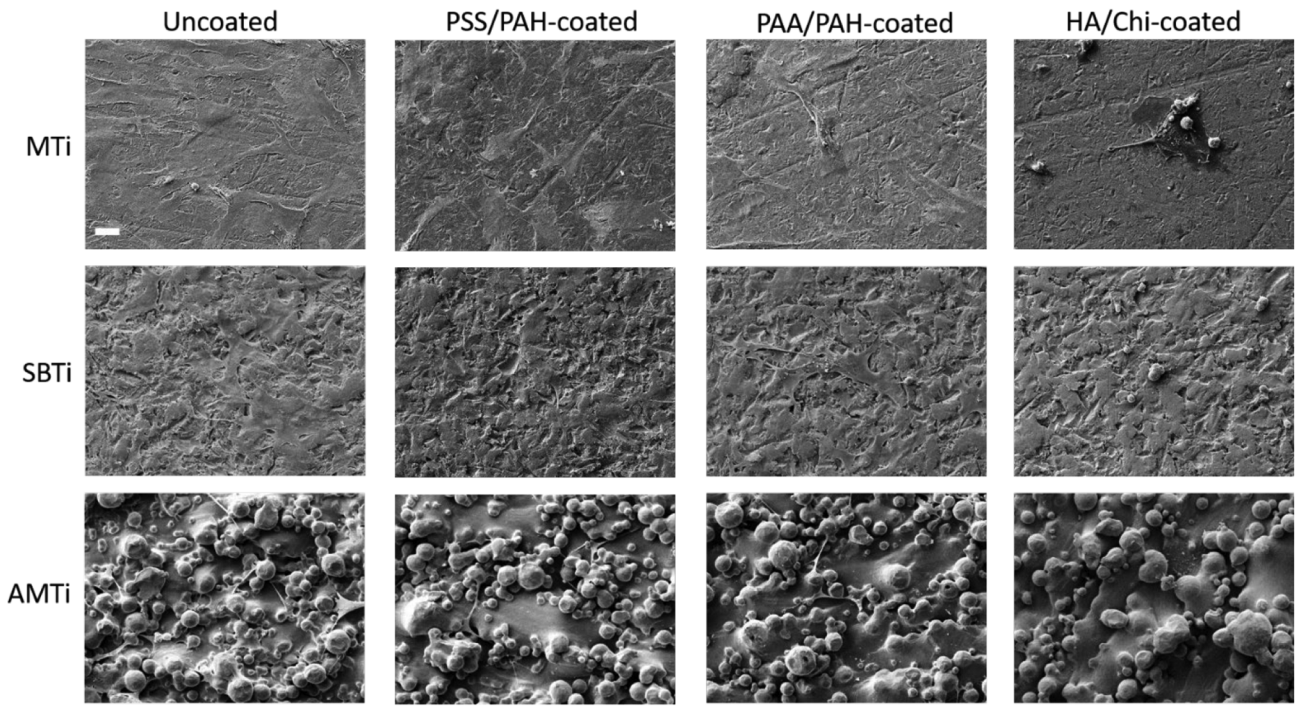

Figure 3. *Scanning electron micrographs representing the morphology of human osteoblasts attached to machined (MTi), sand-blasted (SBTi), and additively manufactured (AMTi) titanium disks uncoated and coated with polystyrene sulfonate (PSS)/polyallylamine hydrochloride (PAH), polyacrylic acid (PAA)/PAH, and hyaluronic acid (HA)/chitosan (Ch) after 24 h of cultivation. Magnification 1,200×, the white bar corresponds to 20 μm.*

by a layer of water molecules, followed by the adsorption of proteins from blood and biological fluids. This protein layer has distinct chemical, physicochemical, and biological properties that facilitate interactions with surrounding tissue cells. The characteristics of the protein layer differ from those of the implanted material, yet they are influenced by it. As a result, the interaction between cells and the implant is significantly mediated and controlled by the adsorbed proteins (40).

Surface charge is a crucial factor influencing protein adsorption and cell adhesion, as both processes are enhanced on positively charged surfaces (41). Uncoated titanium is covered with a layer of TiO_2, which has a slightly negative surface charge at pH 7.4 (the pH of the

buffered HSA solution) (42), potentially explaining the lack of protein adsorption. In contrast, TCP also exhibits a negative surface charge due to the abundance of polar groups, such as hydroxyl and carboxyl, promoting cell adhesion (43) while simultaneously exhibiting the highest surface density of adsorbed HSA (Table IV). All coated Ti_6Al_4V substrates possess a positive surface charge, as they are terminated with polycations.

No correlation was observed between the degree of surface hydrophilicity and the surface density of protein adsorption. The only systematic correlation found here was between the surface chemical composition and the amount of adsorbed HSA. PSS/PAH and PAA/PAH coatings, rich in reactive amino groups, are known to attract negatively charged proteins and DNA at physiological pH (44).

Looking at the surface characteristics of uncoated and PEM-coated Ti substrates it becomes clear that osteoblasts adhesion and proliferation is not controlled by surface hydrophilicity. Majority of studies on cell–material interactions highlight substrate stiffness as a key determinant of cell fate (45). As a general rule, cells adhere to PEMs in direct correlation to their native mechanical properties (46). According to literature data, titanium alloy Ti_6Al_4V [~110GPa, (47)] and TCP [~8GPa, (48)] have much higher Young's modulus than PEM coatings, which range from a few kPa to several hundred MPa depending on their composition. Young's modulus of PSS/PAH multilayers was estimated in the range 130-170 MPa (49), PAA/PAH multilayers assembled at pH 6.5 exhibited a Young's modulus of 153±70MPa (48), and HA/Chi films have been shown to be much softer, with a Young's modulus of only 75 kPa (20). Based on these data, we can conclude that attachment of NHOst on the uncoated and PEM-coated Ti disks was only partly controlled by surface rigidity (Table V). Cells demonstrated the same and, in some cases, even higher affinity for PSS/PAH- and PAA/PAH-coated specimens and uncoated Ti_6Al_4V although the latter has about 1,000 times higher Young's modulus. As expected, the soft HA/Chi film substantially suppressed cell adhesion and proliferation. It seems therefore that there is another surface property besides rigidity that is more effective in controlling osteoblasts behavior. It is important to note that there are interdependencies between surface properties, and altering one affects one or more of the other characteristics (50).

Under the conditions of our study, the quantity of attached cells was generally independent of Sa. While cell proliferation is primarily influenced by surface chemical composition, Sa plays only a minor role. SEM images indicate that the high Sa and the specific micro-structured topography of AMTi strongly modulated cell spreading and morphology, by limiting the points of contact between the cells and the rough surface, which may explain the subsequent reduction in cell proliferation.

The initial adhesive engagement between cells and substrate are driven by electrostatic interaction, so surface chemistry and charge play an important role in it. Both coatings promoting protein adsorption and cell adhesion were terminated with PAH, therefore have surface exposed primary amino groups. Our results are consistent with previous studies reporting that amine coatings can enhance cell attachment, proliferation, and osteogenic differentiation (51, 52) and more specifically that amino-functionalization promotes adhesion and spreading of MC3T3-E1 and rat bone marrow mesenchymal stem cells on pure Ti substrates with nanometer-scale Sa (53, 54). Even more recently, a positive correlation between the surface density of amino groups on a functionalized Ti surface and osteoblast adhesion and growth has been reported (55). Many studies relate cell adhesion to the amount of adsorbed proteins and here we demonstrate that the surface density of HSA increased in the same order as NHOst adhesion.

Conclusion

This study investigated the effect of all possible combinations of two factors: Sa (at three levels: 0.5 μm, 2 μm, and 15 μm) and chemistry (represented by three different polyelectrolyte multilayer coatings) of titanium

surfaces as assessed by the affinity of human osteoblasts to nine modified and three uncoated surfaces. The coatings were nano-thick, nano-smooth, and hydrophilic, imparting their inherent individual chemical and physicochemical properties to the titanium surfaces while preserving their specific morphology and micro-roughness.

Based on the collected data, we conclude that the affinity of NHOst to Ti_6Al_4V surfaces is governed by surface chemistry, increasing in the following order: PSS/PAH-coated>PAA/PAH-coated>uncoated>HA/Chi-coated surfaces. Furthermore, in the context of our study, this affinity was generally statistically independent of Sa. Interestingly, the same ranking of the surfaces was observed in terms of the surface density of the adsorbed human serum albumin. Cell proliferation was mainly controlled by surface chemistry, but also to a lesser extent by Sa. No correlation between surface hydrophilicity, protein adsorption and cell attachment was established.

According to the findings of this study, surface chemical composition is one of the major factors that must be considered in the design of coatings for the biofunctionalization of titanium-based materials. The presence of surface-exposed primary amino groups significantly enhanced the adsorption of HSA and supported the adhesion of osteoblasts.

Funding

The Authors gratefully acknowledge the funding provided by the German Research Foundation (Deutsche Forschungsgemeinschaft, DFG) for the subprojects 1, 2 and 4 within the Research Unit 5250 “Permanent and bioresorbable implants with tailored functionality” (No. 449916462).

Conflicts of Interest

All Authors of the manuscript declare that they have no conflicts of interest.

Authors’ Contributions

Tonya Andreeva: Methodology, writing – original draft, investigation, data curation. Osman Akbas: Investigation, formal analysis. Anne Jahn: Investigation, formal analysis. Andreas Greuling: Supervision, project administration, funding acquisition, conceptualization. Andreas Winkel: Investigation, Data curation. Meike Stiesch: Supervision, funding acquisition. Rumen Krastev: Supervision, project administration, funding acquisition, conceptualization.

References

1 Collins DH: Tissue changes in human femurs containing plastic appliances. The Journal of Bone and Joint Surgery. British volume 36-B(3): 458-463, 1954. DOI: 10.1302/0301-620X.36B3.458
2 Albrektsson T, Brånemark PI, Hansson HA, Lindström J: Osseointegrated titanium implants: requirements for ensuring a long-lasting, direct bone-to-implant anchorage in man. Acta Orthop Scand 52(2): 155-170, 1981. DOI: 10.3109/17453678108991776
3 Kligman S, Ren Z, Chung CH, Perillo MA, Chang YC, Koo H, Zheng Z, Li C: The impact of dental implant surface modifications on osseointegration and biofilm formation. J Clin Med 10(8): 1641, 2021. DOI: 10.3390/jcm10081641
4 Petrini M, Pierfelice TV, D’Amico E, Di Pietro N, Pandolfi A, D’Arcangelo C, De Angelis F, Mandatori D, Schiavone V, Piattelli A, Iezzi G: Influence of nano, micro, and macro topography of dental implant surfaces on human gingival fibroblasts. Int J Mol Sci 22(18): 9871, 2021. DOI: 10.3390/ijms22189871
5 Matos GRM: Surface roughness of dental implant and osseointegration. J Maxillofac Oral Surg 20(1): 1-4, 2021. DOI: 10.1007/s12663-020-01437-5
6 Bhat V, Balaji SS: Surface topography of dental implants. NUJHAS 4(4): 46-54, 2014. DOI: 10.1055/s-0040-1703831
7 Stich T, Alagboso F, Křenek T, Kovářík T, Alt V, Docheva D: Implant-bone-interface: Reviewing the impact of titanium surface modifications on osteogenic processes *in vitro* and *in vivo*. Bioeng Transl Med 7(1): e10239, 2021. DOI: 10.1002/btm2.10239
8 Conforto E, Aronsson BO, Salito A, Crestou C, Caillard D: Rough surfaces of titanium and titanium alloys for implants and prostheses. Materials Science and Engineering: C 24(5): 611-618, 2004. DOI: 10.1016/j.msec.2004.08.004
9 Jemat A, Ghazali MJ, Razali M, Otsuka Y: Surface modifications and their effects on titanium dental implants. Biomed Res Int 2015: 791725, 2015. DOI: 10.1155/2015/791725
10 Czumbel LM, Kerémi B, Gede N, Mikó A, Tóth B, Csupor D, Szabó A, Farkasdi S, Gerber G, Balaskó M, Pétervári E, Sepp R, Hegyi P, Varga G: Sandblasting reduces dental implant failure

rate but not marginal bone level loss: A systematic review and meta-analysis. PLoS One 14(5): e0216428, 2019. DOI: 10.1371/journal.pone.0216428

11 Shah FA, Thomsen P, Palmquist A: Osseointegration and current interpretations of the bone-implant interface. Acta Biomater 84: 1-15, 2019. DOI: 10.1016/j.actbio.2018.11.018

12 Samuel RE, Shukla A, Paik DH, Wang MX, Fang JC, Schmidt DJ, Hammond PT: Osteoconductive protamine-based polyelectrolyte multilayer functionalized surfaces. Biomaterials 32(30): 7491-7502, 2011. DOI: 10.1016/j.biomaterials.2011.06.032

13 Xia J, Yuan Y, Wu H, Huang Y, Weitz DA: Decoupling the effects of nanopore size and surface roughness on the attachment, spreading and differentiation of bone marrow-derived stem cells. Biomaterials 248: 120014, 2020. DOI: 10.1016/j.biomaterials.2020.120014

14 Celik HK, Koc S, Kustarci A, Caglayan N, Rennie AEW: The state of additive manufacturing in dental research - A systematic scoping review of 2012-2022. Heliyon 9(6): e17462, 2023. DOI: 10.1016/j.heliyon.2023.e17462

15 Mendelsohn JD, Yang SY, Hiller J, Hochbaum AI, Rubner MF: Rational design of cytophilic and cytophobic polyelectrolyte multilayer thin films. Biomacromolecules 4(1): 96-106, 2003. DOI: 10.1021/bm0256101

16 Detzel CJ, Larkin AL, Rajagopalan P: Polyelectrolyte multilayers in tissue engineering. Tissue Eng Part B Rev 17(2): 101-113, 2011. DOI: 10.1089/ten.TEB.2010.0548

17 Yadroitsev I, Krakhmalev P, Yadroitsava I: Selective laser melting of Ti6Al4V alloy for biomedical applications: Temperature monitoring and microstructural evolution. J Alloys Compd 583: 404-409, 2014. DOI: 10.1016/j.jallcom.2013.08.183

18 Yan C, Hao L, Yang L, Hussein AY, Designs M, Young PG, Li Z, Li Y: Metal alloys uniform TPMS structures. Chapter 3. In: Triply Periodic Minimal Surface Lattices Additively Manufactured by Selective Laser Melting. 3D Printing Technology Series. Academic Press, Elsevier Ltd, pp. 39-130, 2021.

19 Finger C, Stiesch M, Eisenburger M, Breidenstein B, Busemann S, Greuling A: Effect of sandblasting on the surface roughness and residual stress of 3Y-TZP (zirconia). SN Appl Sci 2(10): 1700, 2020. DOI: 10.1007/s42452-020-03492-6

20 Andreeva TD, Hartmann H, Taneva SG, Krastev R: Regulation of the growth, morphology, mechanical properties and biocompatibility of natural polysaccharide-based multilayers by Hofmeister anions. J Mater Chem B 4(44): 7092-7100, 2016. DOI: 10.1039/C6TB01638C

21 Ladam G, Schaad P, Voegel JC, Schaaf P, Decher G, Cuisinier F: In situ determination of the structural properties of initially deposited polyelectrolyte multilayers. Langmuir 16(3): 1249-1255, 2000. DOI: 10.1021/la990650k

22 Trybała A, Szyk-Warszyńska L, Warszyński P: The effect of anchoring PEI layer on the build-up of polyelectrolyte multilayer films at homogeneous and heterogeneous surface. Colloids Surf A 343: 127-132, 2009. DOI: 10.1016/j.colsurfa.2009.01.039

23 Bradford MM: A rapid and sensitive method for the quantitation of microgram quantities of protein utilizing the principle of protein-dye binding. Anal Biochem 72(1-2): 248-254, 1976. DOI: 10.1016/0003-2697(76)90527-3

24 Winkel A, Dempwolf W, Gellermann E, Sluszniak M, Grade S, Heuer W, Eisenburger M, Menzel H, Stiesch M: Introducing a semi-coated model to investigate antibacterial effects of biocompatible polymers on titanium surfaces. Int J Mol Sci 16(2): 4327-4342, 2015. DOI: 10.3390/ijms16024327

25 Pfaffenroth C, Winkel A, Dempwolf W, Gamble LJ, Castner DG, Stiesch M, Menzel H: Self-assembled antimicrobial and biocompatible copolymer films on titanium. Macromol Biosci 11(11): 1515-1525, 2011. DOI: 10.1002/mabi.201100124

26 Waßmann M, Winkel A, Haak K, Dempwolf W, Stiesch M, Menzel H: Influence of quaternization of ammonium on antibacterial activity and cytocompatibility of thin copolymer layers on titanium. J Biomater Sci Polym Ed 27(15): 1507-1519, 2016. DOI: 10.1080/09205063.2016.1214001

27 Calliess T, Sluszniak M, Winkel A, Pfaffenroth C, Dempwolf W, Heuer W, Menzel H, Windhagen H, Stiesch M: Antimicrobial surface coatings for a permanent percutaneous passage in the concept of osseointegrated extremity prosthesis. Biomed Tech 57(6): , 2012. DOI: 10.1515/bmt-2011-0041

28 Kim Y, Jang JH, Ku Y, Koak JY, Chang IT, Kim HE, Lee JB, Heo SJ: Microarray-based expression analysis of human osteoblast-like cell response to anodized titanium surface. Biotechnol Lett 26(5): 399-402, 2004. DOI: 10.1023/b:bile.0000018258.58314.5c

29 Yaseen M, Cowsill BJ, Lu JR: Characterisation of biomedical coatings. Chapter 6. In: Coatings for Biomedical Applications. Driver M (ed.). Woodhead Publishing Series in Materials. Woodhead Publishing, pp. 176-220, 2012.

30 Mesić M, Klačić T, Abram A, Bohinc K, Kovačević D: Role of substrate type in the process of polyelectrolyte multilayer formation. Polymers (Basel) 14(13): 2566, 2022. DOI: 10.3390/polym14132566

31 Zeiger AS, Hinton B, Van Vliet KJ: Why the dish makes a difference: Quantitative comparison of polystyrene culture surfaces. Acta Biomater 9(7): 7354-7361, 2013. DOI: 10.1016/j.actbio.2013.02.035

32 Gil J, Pérez R, Herrero-Climent M, Rizo-Gorrita M, Torres-Lagares D, Gutierrez JL: Benefits of residual aluminum oxide for sand blasting titanium dental implants: osseointegration and bactericidal effects. Materials (Basel) 15(1): 178, 2021. DOI: 10.3390/ma15010178

33 Wenzel RN: Resistance of solid surfaces to wetting by water. Ind Eng Chem 28(8): 988-994, 1936. DOI: 10.1021/ie50320a024

34 Dowling DP, Miller IS, Ardhaoui M, Gallagher WM: Effect of surface wettability and topography on the adhesion of

osteosarcoma cells on plasma-modified polystyrene. J Biomater Appl 26(3): 327-347, 2011. DOI: 10.1177/0885328210372148
35 Schneider A, Richert L, Francius G, Voegel JC, Picart C: Elasticity, biodegradability and cell adhesive properties of chitosan/hyaluronan multilayer films. Biomed Mater 2(1): S45-S51, 2007. DOI: 10.1088/1748-6041/2/1/S07
36 Muzzio NE, Pasquale MA, Diamanti E, Gregurec D, Moro MM, Azzaroni O, Moya SE: Enhanced antiadhesive properties of chitosan/hyaluronic acid polyelectrolyte multilayers driven by thermal annealing: Low adherence for mammalian cells and selective decrease in adhesion for Gram-positive bacteria. Mater Sci Eng C 80: 677-687, 2017. DOI: 10.1016/j.msec.2017.07.016
37 Keselowsky BG, Wang L, Schwartz Z, Garcia AJ, Boyan BD: Integrin α_5 controls osteoblastic proliferation and differentiation responses to titanium substrates presenting different roughness characteristics in a roughness independent manner. J Biomed Mater Res 80A(3): 700-710, 2007. DOI: 10.1002/jbm.a.30898
38 Stoilov M, Stoilov L, Enkling N, Stark H, Winter J, Marder M, Kraus D: Effects of different titanium surface treatments on adhesion, proliferation and differentiation of bone cells: an *in vitro* study. J Funct Biomater 13(3): 143, 2022. DOI: 10.3390/jfb13030143
39 Rausch MA, Shokoohi-Tabrizi H, Wehner C, Pippenger BE, Wagner RS, Ulm C, Moritz A, Chen J, Andrukhov O: Impact of implant surface material and microscale roughness on the initial attachment and proliferation of primary human gingival fibroblasts. Biology (Basel) 10(5): 356, 2021. DOI: 10.3390/biology10050356
40 Barberi J, Spriano S: Titanium and protein adsorption: an overview of mechanisms and effects of surface features. Materials (Basel) 14(7): 1590, 2021. DOI: 10.3390/ma14071590
41 Metwally S, Stachewicz U: Surface potential and charges impact on cell responses on biomaterials interfaces for medical applications. Mater Sci Eng C 104: 109883, 2019. DOI: 10.1016/j.msec.2019.109883
42 Loosli F, Le Coustumer P, Stoll S: Impact of alginate concentration on the stability of agglomerates made of TiO2 engineered nanoparticles: Water hardness and pH effects. J Nanoparticle Res 17(1): article number 44, 2015. DOI: 10.1007/s11051-015-2863-2
43 Lerman MJ, Lembong J, Muramoto S, Gillen G, Fisher JP: The evolution of polystyrene as a cell culture material. Tissue Eng Part B Rev 24(5): 359-372, 2018. DOI: 10.1089/ten.TEB.2018.0056
44 Wertheimer MR, St-Georges-Robillard A, Lerouge S, Mwale F, Elkin B, Oehr C, Wirges W, Gerhard R: Fabrication and characterization of organic thin films for applications in tissue engineering: emphasis on cell-surface interactions. MRS Online Proc Libr 1469: 2012. DOI: 10.1557/opl.2012.929
45 Macri-Pellizzeri L, De-Juan-Pardo EM, Prosper F, Pelacho B: Role of substrate biomechanics in controlling (stem) cell fate: Implications in regenerative medicine. J Tissue Eng Regen Med 12: 1012-1019, 2018. DOI: 10.1002/term.2586
46 Boudou T, Crouzier T, Auzély-Velty R, Glinel K, Picart C: Internal composition *versus* the mechanical properties of polyelectrolyte multilayer films: the influence of chemical cross-linking. Langmuir 25(24): 13809-13819, 2009. DOI: 10.1021/la9018663
47 Geetha M, Singh AK, Asokamani R, Gogia AK: Ti-based biomaterials, the ultimate choice for orthopaedic implants – A review. Prog Mater Sci 54(3): 397-425, 2009. DOI: 10.1016/j.pmatsci.2008.06.004
48 Thompson MT, Berg MC, Tobias IS, Rubner MF, Van Vliet KJ: Tuning compliance of nanoscale polyelectrolyte multilayers to modulate cell adhesion. Biomaterials 26(34): 6836-6845, 2005. DOI: 10.1016/j.biomaterials.2005.05.003
49 Vinogradova OI, Andrienko D, Lulevich VV, Nordschild S, Sukhorukov GB: Young's modulus of polyelectrolyte multilayers from microcapsule swelling. Macromolecules 37(3): 1113-1117, 2004. DOI: 10.1021/ma0350213
50 Maleki E, Unal O, Reza Kashyzadeh K, Bagherifard S, Guagliano M: A systematic study on the effects of shot peening on a mild carbon steel: Microstructure, mechanical properties, and axial fatigue strength of smooth and notched specimens. Appl Surf Sci Adv 4: 100071, 2021. DOI: 10.1016/j.apsadv.2021.100071
51 Liu X, Feng Q, Bachhuka A, Vasilev K: Surface modification by allylamine plasma polymerization promotes osteogenic differentiation of human adipose-derived stem cells. ACS Appl Mater Interfaces 6(12): 9733-9741, 2014. DOI: 10.1021/am502170s
52 Martocq L, Douglas TEL: Amine-rich coatings to potentially promote cell adhesion, proliferation and differentiation, and reduce microbial colonization: strategies for generation and characterization. Coatings 11(8): 983, 2021. DOI: 10.3390/coatings11080983
53 Yan S, Komasa S, Agariguchi A, Pezzotti G, Okazaki J, Maekawa K: Osseointegration properties of titanium implants treated by nonthermal atmospheric-pressure nitrogen plasma. Int J Mol Sci 23(23): 15420, 2022. DOI: 10.3390/ijms232315420
54 Lu M, Shao D, Wang P, Chen D, Zhang Y, Li M, Zhao J, Zhou Y: Enhanced osteoblast adhesion on amino-functionalized titanium surfaces through combined plasma enhanced chemical vapor deposition (PECVD) method. RSC Adv 6(86): 82688-82697, 2016. DOI: 10.1039/C6RA08922D
55 Seemann S, Dubs M, Koczan D, Salapare HS 3rd, Ponche A, Pieuchot L, Petithory T, Wartenberg A, Staehlke S, Schnabelrauch M, Anselme K, Nebe JB: Response of osteoblasts on amine-based nanocoatings correlates with the amino group density. Molecules 28(18): 6505, 2023. DOI: 10.3390/molecules28186505